

# Inhibitory CA1-CA3-Hilar Region Feedback in the Hippocampus

Attila Sik, Aarne Ylinen,\* Markku Penttonen, György Buzsáki†

The organization of the hippocampus is generally thought of as a series of cell groups that form a unidirectionally excited chain, regulated by localized inhibitory circuits. With the use of *in vivo* intracellular labeling, histochemical, and extracellular tracing methods, a longitudinally widespread, inhibitory feedback in rat brain from the CA1 area to the CA3 and hilar regions was observed. This long-range, cross-regional inhibition may allow precise synchronization of population activity by timing the occurrence of action potentials in the principal cells and may contribute to the coordinated induction of synaptic plasticity in distributed networks.

The cell types of the hippocampus and their network connections have been investigated intensively, for such knowledge is a prerequisite for understanding the involvement of the hippocampus in memory formation, temporal lobe epilepsy, ischemic damage, and Alzheimer's disease (1). Earlier studies revealed a unidirectional feed-forward excitatory pathway from the entorhinal cortex to dentate granule cells to CA3 to CA1 pyramidal cells and subicular neurons (2). The spread of excitation is controlled by local circuit inhibitory interneurons (3). Although recent studies have begun to unveil the complexities of the inhibitory and excitatory circuitries of the hippocampus (3–6), the view that the intrahippocampal flow of information is largely unidirectional has remained unchallenged (7). We describe here a new type of CA1 interneuron that projects back to the CA3 and hilar regions.

In the course of our histochemical experiments with reduced nicotinamide adenine dinucleotide phosphate (NADPH)-diaphorase (8), axon collaterals were frequently observed to cross the hippocampal fissure in both intact and subcortically denervated rats (9). In several cases, axon collaterals emerging from parent cell bodies in the CA1 region could be followed to the hilar region (Fig. 1, A through C). A feature of these axon collaterals was the presence of extremely short (1 to 4  $\mu\text{m}$ ), drumstick-like appendages with large boutons and narrow necks (Fig. 1D). These NADPH-diaphorase-positive neurons are known to contain the synthesizing enzyme of nitric oxide (NO) and are immunoreactive for  $\gamma$ -aminobutyric acid (GABA) (8, 10).

To verify the above observations, we injected a small volume of the anterograde tracer biocytin extracellularly into the

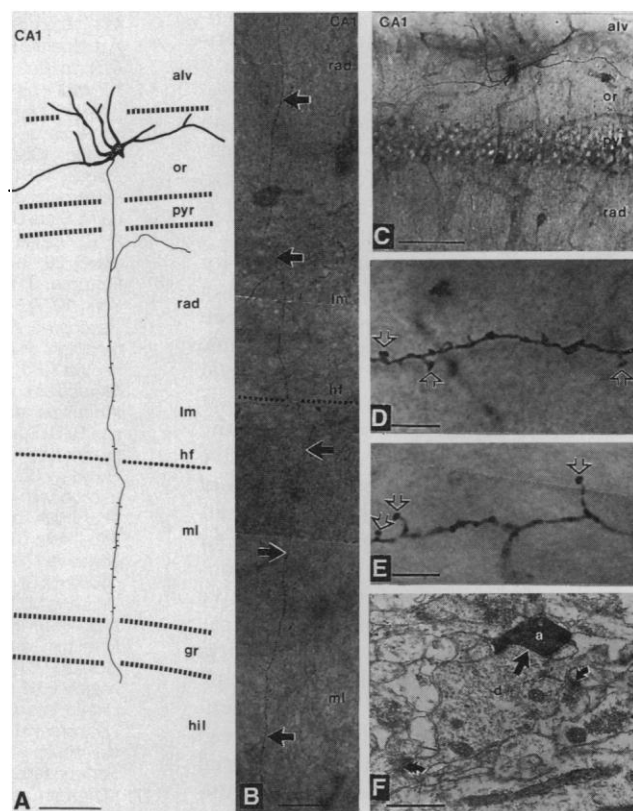
alveus and stratum oriens of the CA1 region (11). Labeled axon collaterals were observed in the stratum radiatum of the CA1 and CA3 areas and in the hilar region in both intact rats and rats with subcortical denervation of the hippocampus (Fig. 2). A typical feature of the axon collaterals entering the CA3 and hilar regions was the presence of drumstick-like appendages.

In the next series of experiments, we impaled, labeled, and reconstructed 12 non-pyramidal neurons in the CA1 region in 162 rats (12). Physiological analysis revealed the typical characteristics of interneurons: fast (10 to 400 Hz), short-duration

action potentials, pronounced spike after hyperpolarization, and limited spike frequency accommodation (13). Six cells were typical basket cells, one of them was a chandelier cell, two of them arborized primarily in the basal and apical dendritic layers (3), and one neuron innervated exclusively the distal apical dendrites of pyramidal cells. Three-dimensional reconstruction of their axon arbors indicated that they were local circuit neurons (3) because axon collaterals concentrated at the level of the cell body with limited (within  $\pm 0.6$  mm) septotemporal spread. Axon collaterals of the remaining two neurons, however, left the CA1 region.

The soma of the first cell was found in the alveus, and its dendrites projected into the stratum oriens (Fig. 3). The dendrites were beaded, and occasional spines were found on the distal dendrites. The principal axon gave rise to six main collaterals, all of which crossed the pyramidal layer. Three of them coursed through the stratum radiatum of the CA3 region, two of them crossed the hippocampal fissure and the granule cell layer, and the sixth remained in the CA1 region. The main collaterals gave rise to rich axon terminal networks in all three regions. On the basis of bouton density [ $24.80 \pm 4.13$  (SD) per 100  $\mu\text{m}^2$ ] and total axonal length (101 mm), we estimated that

**Fig. 1.** (A) Reconstruction of the dendrites and a main axon collateral of an NADPH-diaphorase-positive cell from three neighboring brain sections. Note that the main axon crossed the fissure en route to the hilar region. (B and C) Photomontage of the axon collateral [arrows in (B)] and the cell body (C), respectively. (D and E) "Drumstick-like" axonal appendages (arrows) on the collaterals of the NADPH-diaphorase-positive cell (D) and of the biocytin-labeled neuron (E) shown in Fig. 3. (F) Electron micrograph of the biocytin-filled axon terminal (a) in the CA3 stratum radiatum on a dendritic shaft (d). The straight arrow indicates a symmetric synapse. The same dendrite received an asymmetric synapse on a spinehead (double-headed curved arrow). Another asymmetric synapse is marked by a curved arrow. Size bars: (A), 100  $\mu\text{m}$ ; (B), 25  $\mu\text{m}$ ; (C), 100  $\mu\text{m}$ ; (D) and (E), 5  $\mu\text{m}$ ; and (F), 0.5  $\mu\text{m}$ . Abbreviations: alv, alveus; or, stratum oriens; pyr, pyramidal layer; rad, stratum radiatum; Im, lacunosum-moleculare; hf, hippocampal fissure; ml, molecular layer; gr, granule cell layer; and hil, hilar region.

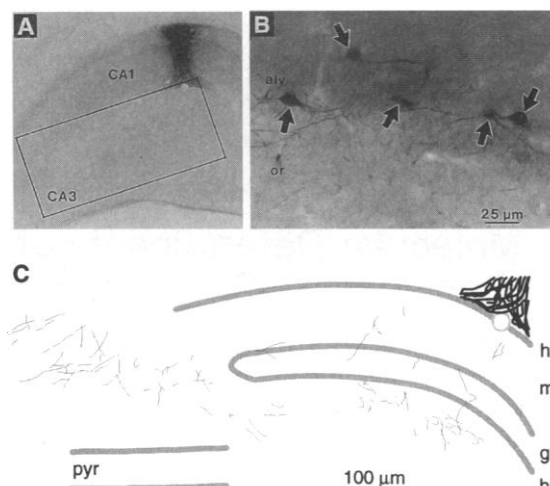


Center for Molecular and Behavioral Neuroscience, Rutgers University, Newark, NJ 07102, USA.

\*Present address: Department of Neurology, University of Kuopio, Kuopio, Finland.

†To whom correspondence should be addressed.

**Fig. 2.** Axon collaterals labeled in an anterograde manner in the CA3 and hilar regions after extracellular injection of biocytin in the CA1 region (17). (A) Injection site. (B) Labeled nonpyramidal cells (arrows) at the stratum oriens–alveus border posterior to the injection site. (C) Enlarged camera lucida drawing of the boxed area shown in (A). Note labeled collaterals in the CA3 and hilar regions in this single 100- $\mu$ m section. The subcortical inputs to the hippocampus had been removed 10 days before the biocytin injection (9). Abbreviations are as in Fig. 1.



this interneuron formed approximately 25,000 synapses within the hippocampus. The physiological characteristics of the cell revealed features of an interneuron (Fig. 4). Similar to the NADPH-diaphorase axon collaterals, drumstick-like appendages were present on the biocytin-labeled axons in all regions and layers (Fig. 1E). Electron microscope examination (14) of the boutons

revealed that the axon collaterals made symmetric synapses on dendritic shafts and cell bodies, but not on the dendritic spines, of unidentified target neurons (Fig. 1F). Spines were often present on the dendrites of several target neurons, which suggests that they were pyramidal cells.

The cell body of the second cell projecting backward (relative to the direction of

**Fig. 3.** Axonal and dendritic arborization of an intracellularly labeled feedback CA1 neuron, reconstructed from 52 60- $\mu$ m coronal sections. The cell body is in the alveus. Axon collaterals were found in three regions of the hippocampus (CA1 = 24.3% of the entire axon length; CA3 = 61.5%; and the dentate hilar region = 14.2%). The dendritic tree resembled somatostatin-immunoreactive and NADPH-diaphorase neurons (10, 20). Thick lines represent the borders of the hippocampus and cell layers. Inset: summated lengths of axon collaterals along the septotemporal axis. S, septal direction; T, temporal direction. Abbreviations are as in Fig. 1.

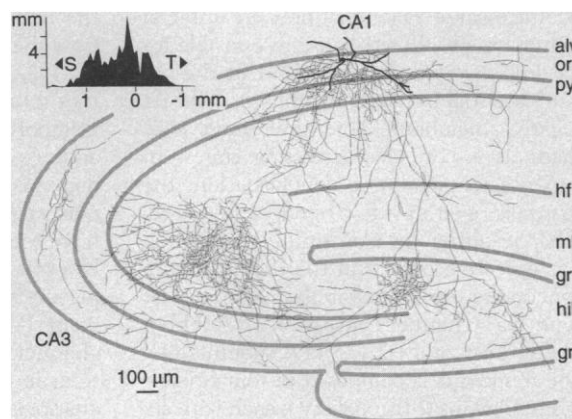
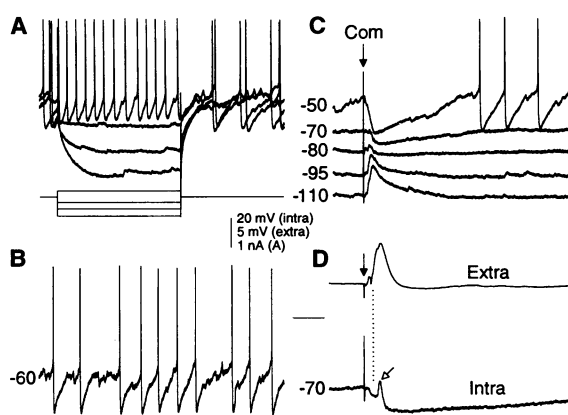


**Fig. 4.** Electrophysiological properties of the neuron shown in Fig. 3. (A) Voltage responses of the cell (upper traces) to depolarizing and hyperpolarizing current steps (lower traces). (B) Spontaneous activity at the resting membrane potential. (C) Evoked responses to commissural path (arrow) stimulation (90  $\mu$ A). Note the polarity reversal of the hyperpolarizing response below  $-70$  mV, which indicates a GABA<sub>A</sub> receptor-mediated synaptic potential (21). (D) At higher intensity (150  $\mu$ A), a depolarizing potential (open arrow) occurred intracellularly 3 ms after the extracellularly recorded population spike (upper trace; dotted line), indicating recurrent excitation of the neuron by CA1 pyramidal cells. The extracellular electrode was placed in the CA1 pyramidal layer. Calibration bar: 50 ms [(A) and (C)]; 100 ms in (B); and 25 ms in (D).



information flow) was at the border of the alveus and stratum oriens. Its long dendrites were confined to the stratum oriens. A rich axon arbor was present in the strata oriens, pyramidale, and radiatum of the CA1 region, covering a 2.2-mm segment in the septotemporal direction. A main axon collateral coursed into the CA3 stratum radiatum, giving off several collaterals in the stratum radiatum of the CA3a and CA3b regions. Another main collateral traveled almost to the septal end of the hippocampus and turned caudally to give rise to a terminal arbor in the CA3 stratum oriens. A third main collateral entered the fornix, where it became myelinated. Drumstick-like appendages were present on the axon collaterals, although they were less numerous than on the other back-projecting interneuron. In contrast, axons of the 10 local circuit interneurons did not have drumstick-like appendages.

The presence of nonprincipal neurons with widespread longitudinal and interregional projection fields should have important implications for the physiological operations and pathophysiological states of the hippocampus. Physiological studies have shown an exceptionally high coherence of population activity in the septotemporal axis of the hippocampus, including theta and gamma waves, irregular sharp waves, ultrafast (200 Hz) transient oscillatory waves, and epileptic patterns (15, 16). The propagation velocity of these patterns in the longitudinal direction and across different subfields is often faster than could be accounted for by the conduction velocity of pyramidal cell axons (16). The fast-conducting interneurons with long-range axonal fields may be critically involved in the timing of action potentials of spatially distant principal neurons (17) and thereby in assisting synchronous discharge and coherent oscillations. Another interesting aspect of these neurons is that they may produce NO, a diffusible second messenger that has recently been implicated in long-term potentiation (18). Because activation of a circumscribed group of CA1 pyramidal cells can discharge the long-range feedback neurons, it may be hypothesized that timed release of NO by their extensive axon collateral system may permit use-dependent modification of concurrently active synapses at successive levels of the hilar region and CA3 and CA1 axis (19).

## REFERENCES AND NOTES

1. L. R. Squire, *Psychol. Rev.* **99**, 195 (1992); J. Engel Jr. et al., *Neurology* **40**, 1670 (1990); W. A. Pulsinelli and J. B. Brierley, *Stroke* **10**, 267 (1979); B. T. Hyman, G. W. Van Hoesen, L. J. Kromer, A. R. Damasio, *Ann. Neurol.* **20**, 472 (1986).
2. P. Andersen, T. V. P. Bliss, K. K. Skrede, *Exp. Brain Res.* **13**, 222 (1971).

3. E. H. Buhl, K. Halasy, P. Somogyi, *Nature* **368**, 823 (1994).
4. X.-G. Li, P. Somogyi, J. M. Tepper, G. Buzsáki, *Exp. Brain Res.* **90**, 519 (1992); X.-G. Li, P. Somogyi, A. Ylinen, G. Buzsáki, *J. Comp. Neurol.* **339**, 181 (1994).
5. D. D. Kunkel, J.-C. Lacaille, P. A. Schwartzkroin, *Synapse* **2**, 382 (1988); P. S. Buckmaster, B. W. Strowbridge, D. D. Kunkel, D. L. Schmiede, P. A. Schwartzkroin, *Hippocampus* **2**, 349 (1992); Z.-S. Han, E. H. Buhl, Z. Lorinczi, P. Somogyi, *Eur. J. Neurosci.* **5**, 395 (1993); K. Halasy and P. Somogyi, *ibid.*, p. 411; A. Gulyas *et al.*, *Nature* **366**, 683 (1993); A. Gulyas, R. Miles, N. Hajos, T. F. Freund, *Eur. J. Neurosci.* **5**, 1729 (1993); N. Tamamaki, K. Abe, Y. Nojyo, *Brain Res.* **452**, 255 (1988); N. Tamamaki and Y. Nojyo, *J. Comp. Neurol.* **291**, 509 (1990); *ibid.* **303**, 435 (1991).
6. A. Sik, M. Tamamaki, T. F. Freund, *Eur. J. Neurosci.* **5**, 1719 (1993).
7. D. G. Amaral and M. Witter, *Neuroscience* **31**, 571 (1989); F. H. Lopes da Silva, M. Witter, P. H. Boeijinga, A. Lohman, *Physiol. Rev.* **70**, 453 (1990).
8. S. R. Vincent and H. Kimura, *Neuroscience* **46**, 755 (1992).
9. The fimbria-fornix, the cingulate bundle, the supracallosal stria and part of the corpus callosum, and the cingulate cortex were removed by aspiration, leaving the dorsal hippocampus completely denervated from its subcortical inputs [G. Buzsáki, F. H. Gage, J. Czopf, A. Björklund, *Brain Res.* **400**, 334 (1987)].
10. H. H. Young, J. B. Furness, A. W. R. Shuttleworth, D. S. Bredt, S. H. Snyder, *Histochemistry* **97**, 375 (1992); J. G. Valtchanoff, R. J. Weinberg, V. N. Kharazia, M. Nakane, H. H. W. Schmidt, *J. Comp. Neurol.* **331**, 111 (1993).
11. Biocytin (3%) was injected extracellularly in the CA1 stratum oriens with micropipettes (resistance, 1 to 2 megohms) by 2.0- $\mu$ A depolarizing current pulses for 15 min in 20 urethane-anesthetized rats. Nine of the rats underwent fimbria-fornix lesion 7 to 20 days before the injection (9).
12. Rats were anesthetized with urethane. Stimulating electrodes were inserted into the ventral hippocampal commissure. Intracellular recording was carried out with glass micropipettes filled with biocytin solution (3% in 1 M potassium acetate; resistance, 60 to 95 megohms). After the physiological properties of the cell were determined, biocytin was injected with depolarizing current pulses (1 to 5 nA) for 5 to 60 min. After 2 to 16 hours, rats were perfused with a fixative (4). The avidin-biotinylated horseradish peroxidase complex reaction was used to visualize the biocytin-filled cells [K. Horikawa and W. Armstrong, *J. Neurosci. Methods* **25**, 1 (1988)]. Axon collaterals were drawn with the aid of a drawing tube (4, 6).
13. J. C. Lacaille, A. Mueller, D. D. Kunkel, P. A. Schwartzkroin, *J. Neurosci.* **7**, 1979 (1987); Y. Kawaguchi, H. Katsumaru, T. Kosaka, C. W. Heizmann, K. Hama, *Brain Res.* **416**, 369 (1987).
14. The sections were treated with 1% OsO<sub>4</sub> for 1 hour, dehydrated, counterstained with uranyl-acetate, and finally embedded in Durcupan (Fluka, Basel, Switzerland). Selected areas were re-embedded for ultrathin sectioning. Serial ultrathin sections were cut and mounted on single-slot Formvar-coated grids and counterstained with lead acetate (6).
15. G. Buzsáki, *Neuroscience* **31**, 551 (1989); T. H. Bullock, G. Buzsáki, M. C. McLune, *ibid.* **38**, 609 (1990); G. Buzsáki, Z. Horváth, R. Urioste, J. Hetke, K. Wise, *Science* **256**, 1025 (1992); A. Ylinen, A. Sik, A. Bragin, G. Jando, G. Buzsáki, *J. Neurosci.*, in press.
16. J. Holtsheimer and F. H. Lopes da Silva, *Exp. Brain Res.* **77**, 69 (1989); G. Buzsáki, M. Hsu, C. Slamka, F. H. Gage, Z. Horváth, *Hippocampus* **1**, 163 (1991).
17. R. J. Douglas and K. A. C. Martin, *Neural Comp.* **2**, 283 (1990); W. W. Lytton and T. J. Sejnowski, *J. Neurophysiol.* **66**, 1059 (1991).
18. T. J. O'Dell, R. S. Hawkins, E. R. Kandel, O. Arancio, *Proc. Natl. Acad. Sci. U.S.A.* **88**, 11285 (1991); E. M. Schuman and D. V. Madison, *Science* **254**, 1503 (1991); D. S. Bredt and S. H. Snyder, *Neuron* **8**, 3 (1992).
19. M. Zhuo, S. A. Small, E. R. Kandel, R. D. Hawkins,

*Science* **260**, 1946 (1993); E. M. Schuman and D. V. Madison, *ibid.* **263**, 532 (1994).

20. R. S. Sloviter and G. Nilaver, *J. Comp. Neurol.* **256**, 42 (1987).
21. R. A. Nicoll, R. C. Malenka, J. A. Kauer, *Physiol. Rev.* **79**, 513 (1990).
22. Supported by NIH, the Human Frontier Science Pro-

gram, the Whitehall Foundation, and the Finnish and the Hungarian academies of sciences (F5531). We thank D. G. Amaral, P. Andersen, T. V. P. Bliss, T. F. Freund, M. Hsu, E. R. Kandel, P. A. Schwartzkroin, J. M. Tepper, and R. Traub for helpful suggestions.

29 December 1993; accepted 10 August 1994

## Molecular Determinants of State-Dependent Block of Na<sup>+</sup> Channels by Local Anesthetics

David S. Ragsdale, Jancy C. McPhee, Todd Scheuer, William A. Catterall

Sodium ion (Na<sup>+</sup>) channels, which initiate the action potential in electrically excitable cells, are the molecular targets of local anesthetic drugs. Site-directed mutations in transmembrane segment S6 of domain IV of the Na<sup>+</sup> channel  $\alpha$  subunit from rat brain selectively modified drug binding to resting or to open and inactivated channels when expressed in *Xenopus* oocytes. Mutation F1764A, near the middle of this segment, decreased the affinity of open and inactivated channels to 1 percent of the wild-type value, resulting in almost complete abolition of both the use-dependence and voltage-dependence of drug block, whereas mutation N1769A increased the affinity of the resting channel 15-fold. Mutation I1760A created an access pathway for drug molecules to reach the receptor site from the extracellular side. The results define the location of the local anesthetic receptor site in the pore of the Na<sup>+</sup> channel and identify molecular determinants of the state-dependent binding of local anesthetics.

Voltage-gated Na<sup>+</sup> channels are integral membrane proteins that are responsible for the initial, rapid depolarization of the action potential in nerve and muscle cells. At negative membrane potentials, most Na<sup>+</sup> channels are in closed, resting states. In response to membrane depolarization, the channels open in a few hundred microseconds, resulting in Na<sup>+</sup> influx through a Na<sup>+</sup>-selective pore, and then convert to a nonconducting inactivated state. The rat brain Na<sup>+</sup> channel consists of  $\alpha$  (260 kD),  $\beta$ 1 (36 kD), and  $\beta$ 2 (33 kD) subunits (1). The  $\alpha$  subunit is composed of four homologous domains (I through IV), each with six  $\alpha$ -helical transmembrane segments (S1 through S6) (2, 3). The  $\alpha$  subunit forms functional channels when expressed in mammalian cells (4, 5) or *Xenopus* oocytes (6), although coexpression of  $\beta$ 1 is required for normal kinetic properties in oocytes (7).

Local anesthetics block Na<sup>+</sup> channels with complex voltage- and frequency-dependent properties that are important for the clinical efficacy of the drugs and that indicate that drug binding is modulated by channel state (8–11). The state-dependence of block can be explained by an allosteric model in which a modulated drug receptor has a higher affinity when channels are open or inactivated than when the channels are resting (8–10). Biophysical evidence is consistent with the hypothesis that this receptor site is on the  $\alpha$  subunit in

the ion-conducting pore and accessible from the cytoplasmic side of the channel (9, 12–15). Determination of the amino acids that form the local anesthetic receptor site is important for understanding the complex action of these drugs. The S6 segment in domain IV (segment IVS6) of Ca<sup>2+</sup> channels and the S6 segment of K<sup>+</sup> channels have been implicated in the binding of pore blockers (16). We used site-directed mutagenesis to examine the function of segment IVS6 of the  $\alpha$  subunit of the Na<sup>+</sup> channel in local anesthetic action. Mutations in IVS6 altered the sensitivity of Na<sup>+</sup> channels to local anesthetics, indicating that amino acids in this region are determinants of the action of these drugs.

Rat brain type IIA Na<sup>+</sup> channels (3) expressed in *Xenopus* oocytes (wild type) (17, 18) were blocked ~40% by 200  $\mu$ M etidocaine, a tertiary amine local anesthetic, when the oocytes were stimulated infrequently (1 pulse per 20 s) (Fig. 1A). This tonic block mainly reflects drug binding to resting channels, the channel state that predominated at the holding potential of –90 mV (8–10). To determine whether amino acids in IVS6 are involved in local anesthetic action, we substituted alanine sequentially for the native amino acids at each position from F1756 to L1776 (Fig. 1A) (18). Alanine was chosen because it changes the size and chemical properties of the residues but has minimal effects on protein secondary structure (19).

Most IVS6 mutants exhibited a 40 to 50%

Department of Pharmacology, University of Washington, Seattle, WA 98195, USA.